Aerosol and Air Quality Research, 15: 2212–2224, 2015

ISSN: 1680-8584 print / 2071-1409 online
doi: 10.4209/aaqr.2015.02.0109

Size Distribution and Optical Properties of Particulate Matter (PM_{10}) and Black Carbon (BC) during Dust Storms and Local Air Pollution Events across a Loess Plateau Site

Wei Pu, Xin Wang*, Xueying Zhang, Yong Ren, Jin-Sen Shi, Jian-Rong Bi, Bei-Dou Zhang

Key Laboratory for Semi-Arid Climate Change of the Ministry of Education, College of Atmospheric Sciences, Lanzhou University, Lanzhou, 730000, China

ABSTRACT

We analyzed the suspended particle size distribution in the range of 0.5 to 10 μm and the optical properties of the particles from March 2007 to December 2010 at a site on the Loess Plateau (SACOL; 35.57°N, 104.08°E; 1965.8 m a.s.l.) about 48 km southeast of the center of Lanzhou. The results indicated that the variation in PM_{10} was much larger in spring than in winter because of frequent dust events or local blowing soil dust during spring. The highest number concentrations of coarse-mode particles were likely attributable to dust events that transported mineral dust or soil dust in the spring season, caused by cold fronts or strong local winds. In contrast, the fine-mode particles that dominated in the cold season at SACOL were probably indicative of anthropogenic sources related to fossil-fuel combustion and biomass burning. The comparison of dust events and anthropogenic air pollution shows a clear distinction of lower PM_{10} with higher B_{ap} for pollution episodes and higher PM_{10} with lower B_{ap} for dust events. These findings suggest that the results in the cold season were likely attributable to light absorption of black carbon, and the coarse mode particles were dominant during dust events in spring.

Keywords: Dust storms; Local air pollutants; Aerosol scattering coefficient; Aerosol absorption coefficient; PM_{10}; Black carbon.

INTRODUCTION

Tropospheric particulate matter (PM_{10}) and black carbon (BC) play key roles in regional and global climate depending strongly on their physical and optical properties (Ramanathan *et al.*, 2001b; Arimoto *et al.*, 2006; Li *et al.*, 2011; IPCC, 2013; Bi *et al.*, 2014). They are very effective at modifying the radiation field by absorbing and scattering solar and thermal radiation (Anderson *et al.*, 2003; Huang *et al.*, 2006a, b; Li *et al.*, 2007; Ramanathan and Carmichael, 2008; Bi *et al.*, 2010; Wang *et al.*, 2010) and altering the precipitation rate and hydrological cycle (Rosenfeld *et al.*, 2001; Ramanathan *et al.*, 2005; Su *et al.*, 2008). The Loess Plateau is located in northwestern China, near the largest and most persistent sources of airborne dust in the world, including the Taklimakan, Gobi, Badain Jaran, and Tengger deserts (Zhang *et al.*, 2003a, b; Xu *et al.*, 2004; Sun *et al.*, 2005; Wang *et al.*, 2008; Igarashi *et al.*, 2011; Che *et al.*, 2013). Dust aerosol, one of the major aerosol types of PM_{10}, is an active component in the climate system (Prospero, 1999; Zhao *et al.*, 2008). Driven by midlatitude prevailing westerlies, large quantities of mineral particles can be lifted to high altitudes during dust events and thus transported to the eastern Pacific and North America (Jaffe *et al.*, 1999; Prospero, 1999; VanCuren and Cahill, 2002; Huang *et al.*, 2008a; Prospero and Mayol-Bracero, 2013). Additionally, the region also has major sources of anthropogenic aerosols produced by human activities (Chen *et al.*, 2014; Huang *et al.*, 2014). For instance, BC, which originates from incomplete combustion, is an anthropogenic substance capable of damaging human health and leading to serious climatic effects at scales from regional to global (Ramanathan and Carmichael, 2008; Huang *et al.*, 2011; Wang *et al.*, 2013; Zhang *et al.*, 2013). It is also the strongest absorber of solar radiation, thus contributing to warming of the atmosphere. Additionally, BC affects climate by indirect effects due to its action on cloud droplets and cloud microphysical properties. When BC mixes with dust aerosols during dust events, it significantly changes the aerosol physical and optical properties (Ramanathan *et al.*, 2001a; McKendry *et al.*, 2008; Fu *et al.*, 2009; Zhou *et al.*, 2013; Wang *et al.*, 2015). Therefore, understanding the physical processes and optical properties of aerosol particulates across the Loess Plateau is important (Tegen *et al.*, 1996; Liu *et al.*, 2011).

* Corresponding author.
Tel.: +86-931-8915-892
E-mail address: wxin@lzu.edu.cn

Recently, extensive ground-based and airborne-based measurement campaigns have been conducted to measure the properties of Asian aerosols. These include the Asian Pacific Regional Aerosol Characterization Experiment (ACE-Asia) (Anderson *et al.*, 2003; Conant *et al.*, 2003; Arimoto *et al.*, 2006; Sullivan *et al.*, 2007), the East Asian Study of Tropospheric Aerosols: an International Regional Experiment (EAST-AIRE) (Anderson *et al.*, 2003; Huebert *et al.*, 2003; Zhang *et al.*, 2003b; Arimoto *et al.*, 2004; Kim *et al.*, 2005; 2006), the Transport and Chemical Evolution over the Pacific (TRACE-P) aircraft mission (Jacob *et al.*, 2003; Tu *et al.*, 2003; Woo *et al.*, 2003; Allen *et al.*, 2004; Mari *et al.*, 2004), the Intercontinental Chemical Transport Experiment-Phase B (INTEX-B) campaign (McKendry *et al.*, 2008; Zhang *et al.*, 2009), and the Pacific Dust Experiment (PACDEX) (Huang *et al.*, 2008a). Although there has been much progress in measuring the physical and optical properties of dust and non-dust aerosols (Cao *et al.*, 2014; Jing *et al.*, 2015), the monthly and seasonal variations in these aerosols have yet to be well quantified, especially across the Loess Plateau, near the dust sources. This is due mainly to the aerosols' large variability and complexity in terms of sources, transport and transformation, chemical, optical, and physical properties, and interaction with other components of the climate system (IPCC, 2013).

To recognize aerosol effects on the regional and global climate, variations in the light scattering coefficient, light absorption coefficient, size distribution, and mass concentrations of PM_{10} and BC were investigated from March 2007 to December 2010 at the Semi-Arid Climate and Environment Observatory of Lanzhou University (SACOL), which is 48 km southeast of Lanzhou. Our overall goal was to focus on air pollutants characterized by high concentrations of PM_{10} mixed with BC related to mineral dust, fossil fuel, and biomass burning across the Loess Plateau. In this paper, we first outlined the major objective of this study in the introduction section. Next, in section 2, we describe the experimental measurements and provide details of the data procedures. In section 3, we present the results of the seasonal variations in aerosol scattering and absorption properties at specific wavelengths, the mass concentration of BC, and the number concentration of PM_{10} during this field campaign. We also provide a preliminary characterization of the optical properties of aerosols dominated by dust events and anthropogenic air pollutants. Section 4 is a summary of the conclusions of this study.

DATA AND METHODS

Site Description

The remote observation site SACOL (35.57°N, 104.08°E, 1965.8 m a.s.l.) has been in operation since 2005 (Huang *et al.*, 2008b; Wang *et al.*, 2015). SACOL is located on the Loess Plateau at the western edge of the Hexi Corridor in Gansu Province (south of the Yellow River), about 48 km southeast of central Lanzhou. The motivation for establishing this site was to develop a deeper understanding of the physical and optical properties of PM_{10} and BC in the semi-arid and arid regions near the border of the Loess Plateau and to investigate the impacts of natural and anthropogenic pollution on the regional climate (An *et al.*, 2007; Costabile *et al.*, 2010; Zhang and Li, 2011; Zheng *et al.*, 2013). The characteristic ecosystems at SACOL include various types of vegetation, such as needle-leaf tree, short grass, meadow, marsh/desert, marsh/semi-desert, irrigated crop, and glacier/snow.

Instrumentation

Since March 2007, the mass concentration of PM_{10} has been measured continuously by an R&P1400a analyzer based on the principle of the tapered element oscillating microbalance (TEOM) with the appropriate sample inlet. The instrument works at 50°C in order to dry the aerosols, with a flow rate of 16.7 L min^{-1}. Aerosol scattering coefficient measurement was performed using single-wavelength ECOTECH integrating nephelometers (M9003). The nephelometer was available at the wavelengths of 450, 520, and 700 nm and was designed specifically for studies of the direct radiative forcing of the Earth's climate by aerosol particles or studies of ground-based or airborne atmospheric visual air quality. A seven-wavelength Aethalometer™ (Magee Scientific, model AE-31), described by Fialho *et al.* (2005), was used to measure the concentration of BC in units of ng m^{-3} at the wavelengths of 370, 470, 520, 590, 660, 880, and 990 nm at 5-min intervals from March 2007 to November 2008. We also used multiangle absorption photometer (MAAP) instruments to measure the concentration of BC at the wavelengths of 450, 500, and 700 nm from September 2009 to December 2010. Although we measured the concentration of BC with two different instruments, the outputs provided very comparable results (Hyvärinen *et al.*, 2011). A comparison of values before and after a filter change showed that the aerosol light absorption is reduced by filter multiple scattering enhancement factors (Arnott *et al.*, 2005). The light absorption coefficient (B_{ap}) at the given wavelength of 520 nm was calculated using $B_{ap} = m_{BC} \times 10$ m^2 g^{-1} by assuming a specific absorption efficiency of BC of 10 m^2 g^{-1}, which is supported by Li *et al.* (2010) and Wang *et al.* (2015). In this study, the single scattering coefficient (SSA) was derived using the scattering coefficient and the absorption coefficients at the wavelength of 520 nm. Angstrom (1929) reported that the spectral dependence of extinction by particles could be expressed as a power law relationship:

$$\tau(\lambda) \propto \lambda^{-Å}, \quad (1)$$

where $\tau(\lambda)$ is the aerosol optical thickness (AOT) at the wavelength λ and Å is the Ångstrom exponent. According to the relationship, the corresponding Å is calculated from the slope of the linear regression of the logarithm of the equation:

$$\ln\tau(\lambda) = \beta - Å\ln\lambda.. \quad (2)$$

Then, using the method of least squares, the scatter Ångstrom exponent (SAE) and absorption Ångstrom exponent (AAE) are obtained. The number concentrations

of fine-mode ($0.5 < D_p \leq 1$ μm, hereafter $N_{0.5-1}$) and coarse-mode ($1 < D_p \leq 10$ μm, N_{1-10}) particles were measured continuously using a 51-size channel aerodynamic particle sizer spectrometer (APS, Model 3321) with optical diameter in the range of 0.5–20 μm. Here, the size range was selected as 0.5 to 10 μm due to the detection limit of the APS and the large uncertainty of particle number concentration at sizes beyond 10 μm.

RESULTS AND DISCUSSION

Temporal Variability of Aerosol Properties

Daily averaged aerosol scattering coefficients and aerosol absorption coefficients at the wavelength of 520 nm as well as PM_{10} concentrations at SACOL from March 2007 to December 2010 are shown in Fig. 1; the statistical analyses are summarized in Table 1. Generally, the daily averaged B_{sp}, B_{ap}, and PM_{10} were 155 ± 102 Mm^{-1} (hereafter, related results are shown by mean ± standard deviation), 16 ± 10 Mm^{-1}, and 120 ± 122 μg m^{-3}, respectively; these are much lower than the average values in Beijing, which are in the range of 488 ± 370 Mm^{-1} for B_{sp} and 83 ± 40 Mm^{-1} for B_{ap}, respectively (Bergin *et al.*, 2001). We found high concentrations of PM_{10} from November to February and from March to May, with average values of 121 ± 68 μg m^{-3} and 163 ± 199 μg m^{-3}, respectively. The variation in PM_{10} was much larger in spring than in winter because of frequent dust events or local blowing soil dust during spring (Littmann, 1991; Wang *et al.*, 2008, 2015). The daily maximum PM_{10} could exceed 2519 μg m^{-3} during dust events in spring. Previous studies have indicated that fossil fuel and biomass burning occur more dominantly from November to February (hereafter referred to as the cold season) over northern China, resulting in serious local air pollution (Wang *et al.*, 2004; Sun *et al.*, 2005; Li *et al.*, 2007; Yuan *et al.*, 2008). The maximum values of B_{sp} and B_{ap} were 894 Mm^{-1} and 85 Mm^{-1}, and the average values were 240 ± 145 Mm^{-1} and 26 ± 13 Mm^{-1}, respectively. Although the concentration of PM_{10} was highest in March–

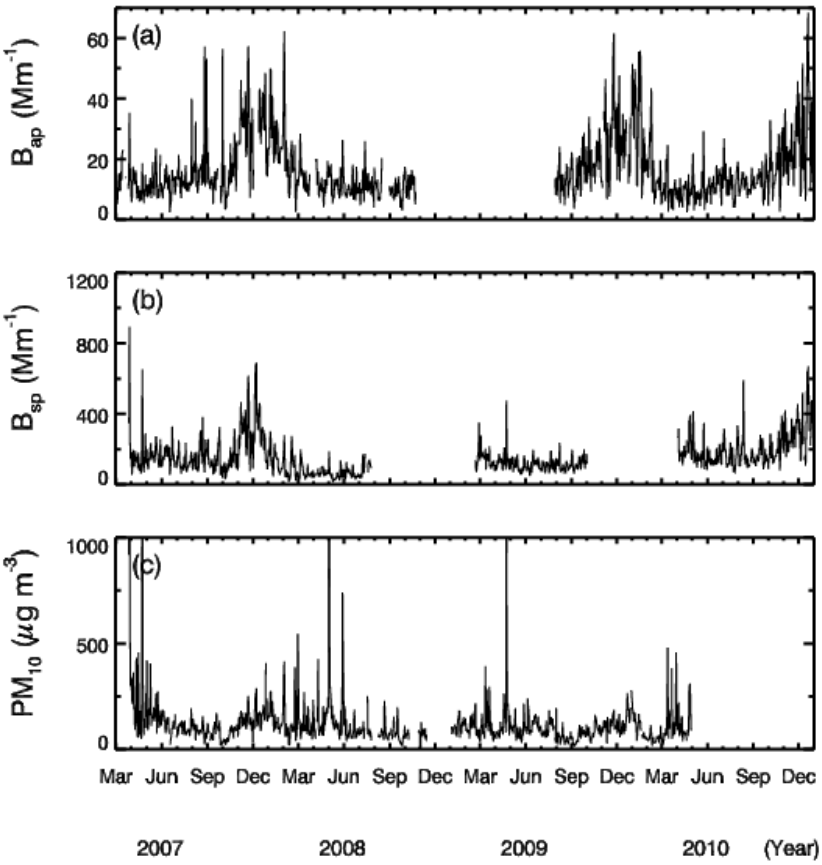

Fig. 1. Variations in daily averages of (a) aerosol absorption coefficient (B_{ap}) at 520 nm, (b) aerosol scattering coefficient (B_{sp}) at 520 nm, and (c) PM_{10} concentration at SACOL from March 2007 to December 2010.

Table 1. Statistics based on measured aerosol optical properties obtained during the field experiment.

	All periods	Mar–May	Jun–Oct	Nov–Feb
PM_{10} (μg m^{-3})	120 ± 122	163 ± 199	86 ± 40	121 ± 68
B_{sp} (Mm^{-1})	155 ± 102	121 ± 89	136 ± 66	240 ± 145
B_{ap} (Mm^{-1})	16 ± 10	11 ± 5	14 ± 7	26 ± 13
SSA	0.90 ± 0.06	0.89 ± 0.07	0.91 ± 0.04	0.88 ± 0.07

May of all seasons, the values of B_{sp} and B_{ap} did not significantly increase and were only about half those in the cold season. Li *et al.* (2010) indicated similar results at the National Climate Observatory of the China Meteorological Administration (39.082°N, 100.276°E; 1,460 m a.s.l.), which is located ~20 km northwest of Zhangye, Gansu Province. As a result, we conclude that the variations in B_{sp} and B_{ap} were not only determined by PM_{10} but also depended on the particle size distribution and the compositions of chemical species (Hegg *et al.*, 2009, 2010). Statistically, the values of B_{sp}, B_{ap}, and PM_{10} were much smaller in the period of June to October (hereafter, the warm season) because of more rainfall in this season.

Fig. 2(a) shows the seasonal variations in the aerosol number concentrations of $N_{0.5–1}$ and $N_{1–10}$ ($0.5\ \mu m < D_p \leq 1\ \mu m$ and $1\ \mu m < D_p \leq 10\ \mu m$, respectively). The seasonal variations in $N_{0.5–1}$ and $N_{1–10}$ exhibited a seasonal cycle of higher concentrations in the cold season, with maximum values of 787 # cm^{-3} and 140 # cm^{-3}, compared with lower concentrations in the warm season, with minimum values of 3.9 # cm^{-3} and 0.8 # cm^{-3}, respectively. Both $N_{0.5–1}$ and $N_{1–10}$ increased remarkably in the cold season, and the number concentration of $N_{0.5–1}$ increased three times more than did that of $N_{1–10}$. Obviously, the fine-mode particles were dominant in the cold season at SACOL, reflecting the role of local air pollutants originating from fossil fuel and biomass burning in the rural and remote regions. For the coarse-mode particles, $N_{1–10}$ was not only very high in the cold season but also remained at its highest number concentration in spring, which is characterized by local soil dust or dust events. Gong *et al.* (2003) noted that ~252.8 Mt of soil dust was estimated to have been produced in the East Asian deserts in a spring season, with ~60% of this being due to four major dust storms. When dust storms occur over northern China, $N_{1–10}$ can increase sharply. These results showed good agreement with those of previous studies (Mori *et al.*, 2003; Marinoni *et al.*, 2008). In Fig. 2(b), the number concentration of $dN/dlogD_p$ showed a prominent seasonal cycle with a daily averaged maximum value of 4040 # cm^{-3} at 0.72 µm. During this field campaign, fine-mode particles with diameters less than 2 µm were dominant in this area, even during strong dust-event periods. The $dN/dlogD_p$ dropped dramatically along with the particle size distribution when the particle size was greater than 5 µm. Previous studies showed that the $dN/dlogD_p$ with particle diameters of 2–5 µm almost reached its highest values during dust events, suggesting that dust events make a great contribution to the increase in particle number concentration of coarse-mode particles (Bi *et al.*, 2013; Huang *et al.*, 2014).

The annual variations in BC concentration and $N_{0.5–1}$ are presented in Fig. 3. The boxes and whiskers denote the 10th, 25th, 50th (median), 75th, and 90th percentiles of the data, with dots marking average values. The BC concentration in this campaign was measured by AE-31 and MAAP from

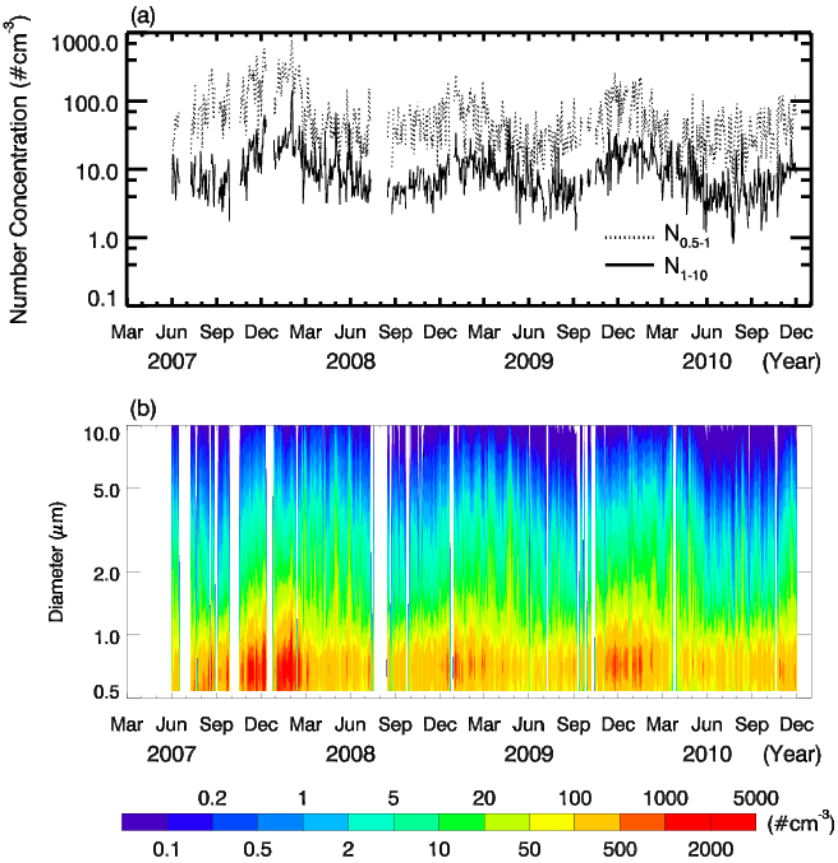

Fig. 2. Daily average variations in the number concentrations of (a) fine-mode ($N_{0.5–1}$) and coarse-mode ($N_{1–10}$) particles and (b) $dN/dlogD_p$ ($0.5\ \mu m < D_p \leq 10\ \mu m$) at SACOL from March 2007 to December 2010.

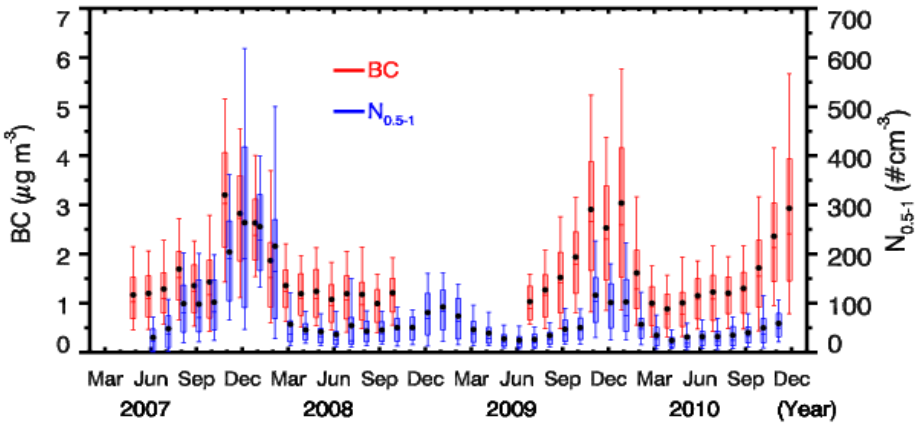

Fig. 3. Seasonal variations in BC concentration and the number concentration of fine-mode particles ($N_{0.5–1}$) at SACOL from March 2007 to December 2010.

May 2007 to October 2008 and from July 2009 to December 2010, respectively. The average value of BC in this campaign was 1.62 ± 1.22 μg m^{-3}. The monthly median BC concentration presented an obvious seasonal cycle, with higher values during the cold season and lower values during the warm season. The maximum cold season value was 3.03 μg m^{-3}, and the minimum warm season value was 0.78 μg m^{-3}. The results indicate that the emissions of BC originated mostly from coal and biomass burning during the cold season. For comparison, the monthly median $N_{0.5–1}$ reached its highest value of 228 # cm^{-3} with larger variation in the cold season, and reached its lowest value of 17.5 # cm^{-3} in the warm season. Especially, there was a positive linear correlation between the daily average BC concentration and $N_{0.5–1}$ (R^2 = 0.52) at the 99% confidence level, implying very similar emission sources (Marinoni *et al.*, 2008). The average values of BC and $N_{0.5–1}$ were larger (3–30%, 8–130%) than the median values, indicating that high air pollution was a large fraction of the contribution of BC and $N_{0.5–1}$ during the field campaign from March 2007 to December 2010. It was very interesting that the ratios of monthly averaged BC during June 2007 to February 2008 to the relative monthly averaged BC during July 2009 to November 2010 were 0.74 to 1.41 (1.08 ± 0.21: mean and standard deviation). However, the ratios of $N_{0.5–1}$ were in the range of 0.93 to 3.8 (average of 2.34 ± 0.77) and especially up to 1.76–3.8 in the cold season (average of 2.83 ± 0.82). The reason could be the limitation of industrial emissions to improve air quality. The number concentration of $N_{0.5–1}$ decreased significantly as a fraction of 36% in the cold season, and the potential reason could be concluded as the limitation of industrial emissions to improve air quality (An *et al.*, 2007; Coatabile *et al.*, 2010; Zheng *et al.*, 2013). However, the concentration of BC, originating from biomass and fossil-fuel burning, was even higher in the cold season of 2009.

Seasonal Variations of Aerosol Properties

The averaged diurnal variations in B_{ap}, B_{sp}, SSA, and PM_{10} over three periods are shown in Fig. 4. The minimum concentration of PM_{10} was recorded during daytime at about 16:00 because of the strong vertical convection at that time. There were two peaks of concentration, whose timing varied in the different periods (Mar–May: 8:00 and 21:00, Jun–Oct: 8:00 and 19:00, Nov–Feb: 10:00 and 20:00) with average concentrations of 181.6 and 178.8, 104.0 and 93.8, and 149.0 and 125.5 μg m^{-3}, respectively. Generally, the concentration of PM_{10} was higher in spring than in the other periods. Due to biomass and coal burning resulting in serious anthropogenic emissions, the concentration of PM_{10} in winter was only lower than that in spring. The result agrees well with those of previous studies (Bi *et al.*, 2010; Wang *et al.*, 2010, 2015; Che *et al.*, 2014). As for PM_{10}, the diurnal cycle of B_{ap} presented two peaks (Mar–May: 8:00 and 21:00, Jun–Oct: 8:00 and around 20:00–23:00, Nov–Feb: 10:00 and 20:00), with average values of 15.3 and 11.2, 17.8 and 14.3, and 32.1 and 28.3 Mm^{-1}. Compared with the relatively low PM_{10} concentration during the cold season, B_{ap} was highest in the cold season, which can be explained easily because biomass and coal burning produced large amounts of light-absorbing aerosols, especially BC which has the ability to absorb visual light greater than that of the dust particles that were predominant in spring. The variation in B_{sp} was consistent with that in B_{ap}, with peaks of 248 and 290 Mm^{-1}, 156 and 129 Mm^{-1}, and 171 and 132 Mm^{-1} in the cold season, spring, and warm season, respectively. The single-scattering albedo (SSA), defined as the ratio of scattering efficiency to total extinction efficiency, is a key parameter for investigating aerosol optical properties. During this field campaign, the SSA showed a trend opposite to the peaks of B_{ap} and B_{sp}. The SSA was lowest in the cold season due to more light-absorbing aerosols from biomass and coal burning, with two valley values of 0.87 at 10:00 and 20:00–23:00, and with a maximum value of 0.89. The SSA was largest in the warm season, with values ranging from 0.89 to 0.91, suggesting the lowest amount of light-absorbing aerosols relative to light-scattering particles during this period.

The seasonal average size distributions of the fine and coarse modes were calculated from March 2007 to December 2010, as shown in Fig. 5. The highest averaged $dN/dlogD_p$ occurred with particle size distributions in the range of 0.5

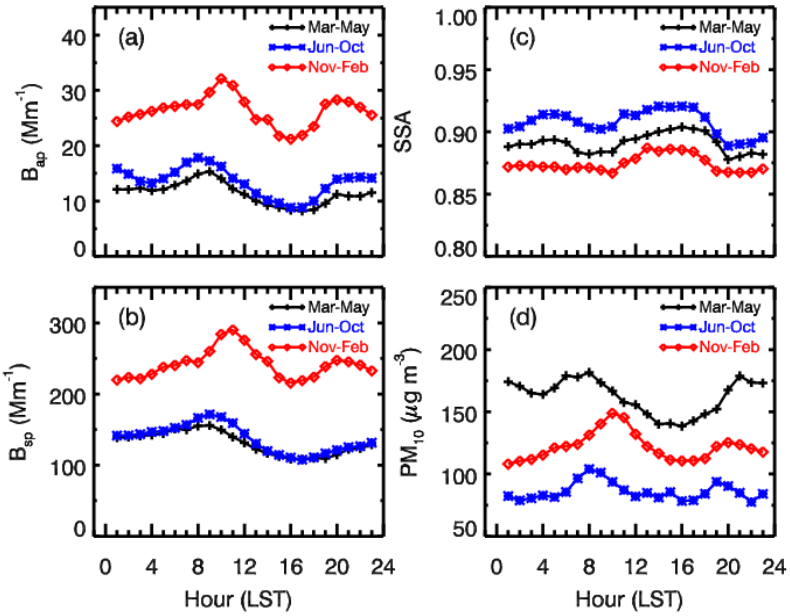

Fig. 4. Diurnal variations of (a) B_{ap}, (b) B_{sp}, (c) single scattering albedo (SSA), and (d) PM_{10} concentration at SACOL for the periods March–May, June–October, and November–February.

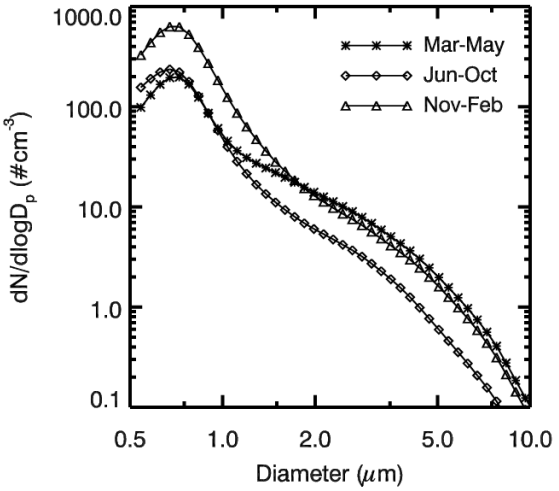

Fig. 5. Seasonal variations in the aerosol number concentration of $dN/dlogD_p$ ($0.5\ \mu m < D_p \leq 10\ \mu m$) at SACOL for the periods March–May, June–October, and November–February.

to 1.84 μm in the cold season and 1.84 to 10 μm in spring. The peak values of $dN/dlogD_p$ were 198 # cm^{-3} at 0.72 μm in spring, 237 # cm^{-3} at 0.67 μm in the warm season, and 632 # cm^{-3} at 0.67 μm in the cold season. $dN/dlogD_p$ with diameter larger than 1.84 was a little higher in spring compared with the other two periods because of the influence of local blowing soil dust and frequent dust storms. As shown in Fig. 5, the trend of $dN/dlogD_p$ with particle size over the whole range was similar between the warm and cold seasons, reflecting the similar emission sources. The difference in the trends was that the aerosol emission in spring had considerably more large particles compared with the abundant fine-mode particles in the cold season, which was dominated by emissions from fossil-fuel and biomass burning for heating. Although the PM_{10} concentration in the cold season was not the highest, the particle number concentration of light-absorbing aerosols was much higher than in the other periods. As a result, both B_{ap} and B_{sp} showed their highest values in the cold season. Comparing the spring and warm seasons, a pattern shift appeared at the size of 0.97 μm (near 1 μm), and the value of $dN/dlogD_p$ from 0.5 to 0.97 μm was a little higher in the warm season. The higher aerosol number concentration during the warm season may be related to the amount of anthropogenic emissions, such as industrial emissions and emissions from fuel burning, and to the fact that the nature of the emissions in spring, originating from local blowing soil dust and frequent dust storms, made a primary contribution to coarse-mode aerosols but had only a limited effect on fine-mode aerosols. Additionally, the result of light-absorbing particles, such as BC and OC, with sizes below 1 μm has already been discussed in previous studies (Petzold *et al.*, 1997; Hitzenberger and Tohno., 2001).

Comparison of Aerosol Properties of Dust Events and Air Pollutants

Six cases each of dust events and anthropogenic air pollution events were selected to further examine their characteristics (Figs. 6 and 7). The statistical analyses of these events are summarized in Table 2. As shown in Fig. 6(a), the time series of PM_{10} during the dust events were different and varied due to the meteorological conditions and the intensity of the dust emission sources. The dust events occurred at various times of the day, and their durations varied from several hours to dozens of hours. For example, the hourly averaged PM_{10} at 14:00 (local time) on 29 February 2008 was around 100 μg m^{-3}, but the PM_{10} then increased sharply, with large intensity but short duration, to its peak value of 2078 μg m^{-3}, nearly 20 times higher than

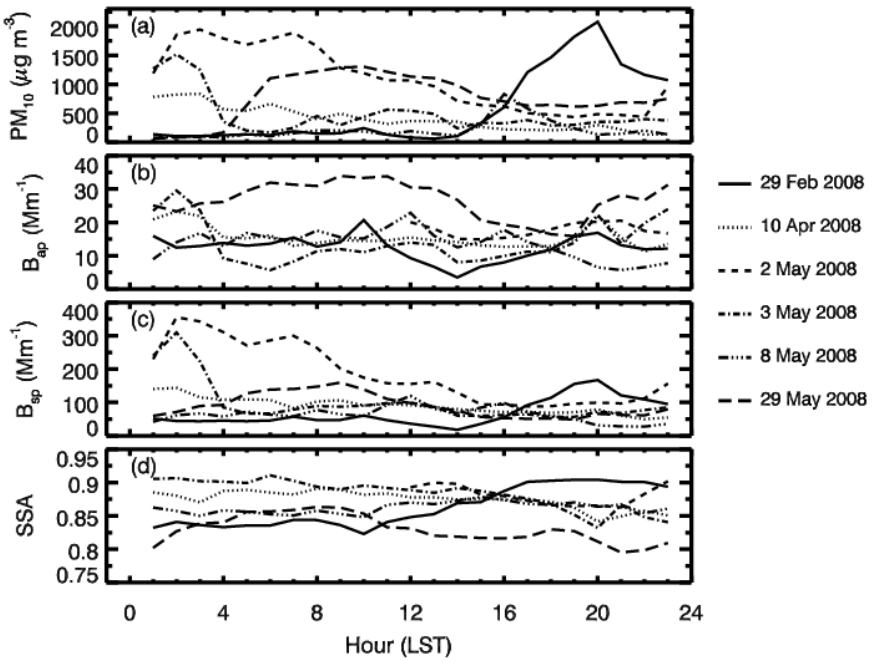

Fig. 6. Hourly average variations in (a) PM_{10} concentration, (b) B_{ap}, (c) B_{sp}, and (d) SSA at SACOL during dust events from March 2007 to December 2010.

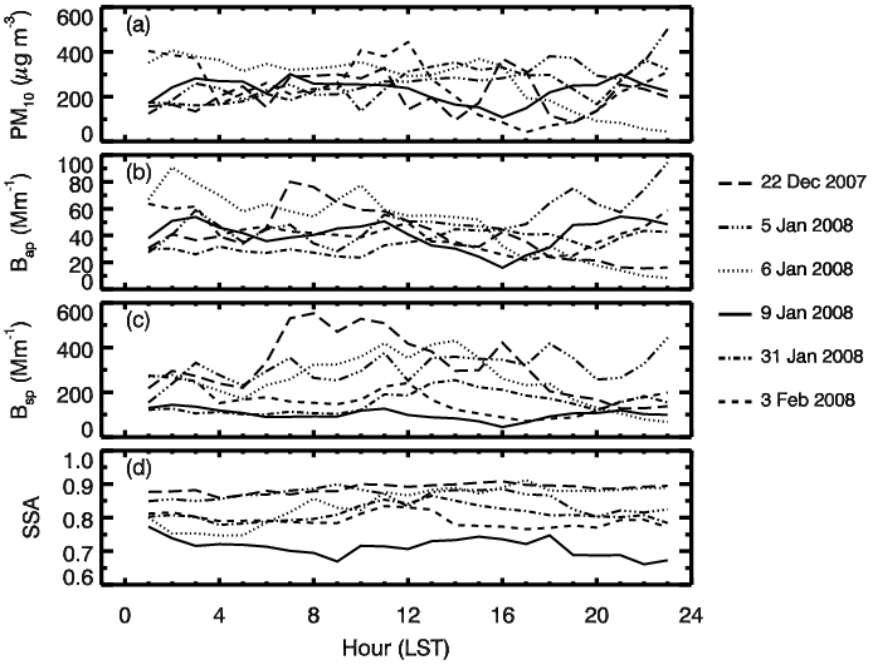

Fig. 7. Hourly average variations in (a) PM_{10} concentration, (b) B_{ap}, (c) B_{sp}, and (d) SSA at SACOL during local air pollution events from March 2007 to December 2010.

the value before the dust storm occurred. For another case occurring on 2 May 2008, two peak concentrations of PM_{10} of 1945 μg m^{-3} and 1889 μg m^{-3} occurred at 3:00 and 7:00, respectively; then, the concentration of PM_{10} decreased slowly to the minimum value of 434 μg m^{-3} at 19:00. At 2:00 on 3 May 2008, the PM_{10} concentration increased to its peak value of 1519 μg m^{-3} after a few hours. However, these two nearly continuous dust events (2 and 3 May; intervals of only a few hours) originated from different emission sources according to the 60-h HYSPLIT air-mass back trajectories (Kalkstein *et al.*, 1987; Stunder, 1997; Draxier and Hess, 1998; Draxler and Rolph, 2008; Huang *et al.*, 2008a; Zhang *et al.*, 2013). These air-mass back trajectories have been considered by previous studies to be an effective method of tracking the transport of dust events (Zhang *et al.*, 2003a, b; Huang *et al.*, 2010; Chen *et al.*, 2013) and have been

Table 2. Statistics of aerosol optical properties observed during local air pollution and dust events.

	Date	Time (LST)	PM_{10} (μg m^{-3})	B_{sp} (Mm^{-1})	B_{ap} (Mm^{-1})	SSA
Pollution episodes						
Case 1	22-Nov-07	1:00–23:00	212 ± 81	315 ± 137	40 ± 18	0.89 ± 0.01
Case 2	5-Jan-08	1:00–23:00	273 ± 78	309 ± 66	51 ± 16	0.86 ± 0.03
Case 3	6-Jan-08	1:00–19:00	314 ± 70	291 ± 81	56 ± 18	0.83 ± 0.06
Case 4	9-Jan-08	1:00–23:00	230 ± 51	101 ± 23	41 ± 10	0.71 ± 0.03
Case 5	31-Jan-08	1:00–23:00	248 ± 72	154 ± 48	34 ± 7.0	0.91 ± 0.02
Case 6	3-Feb-08	1:00–23:00	241 ± 119	163 ± 59	42 ± 12	0.79 ± 0.02
Dust events						
Case 1	29-Feb-08	17:00–23:00	1451 ± 371	122 ± 29	13.1 ± 2.4	0.90 ± 0.01
Case 2	10-Apr-08	1:00–20:00	444 ± 204	95 ± 22	15.8 ± 3.4	0.86 ± 0.02
Case 3	2-May-08	1:00–23:00	1092 ± 547	186 ± 90	17.7 ± 2.1	0.86 ± 0.03
Case 4	3-May-08	1:00–6:00	794 ± 616	165 ± 105	16.5 ± 10.2	0.91 ± 0.01
Case 5	8-May-08	15:00–19:00	466 ± 243	73 ± 19	13.5 ± 1.0	0.84 ± 0.01
Case 6	29-May-08	5:00–23:00	910 ± 265	92 ± 39	27.0 ± 6.0	0.76 ± 0.04

applied in deserts such as the Taklimakan (Li *et al.*, 2007; Huang *et al.*, 2008a; Wang *et al.*, 2008; Zhou *et al.*, 2013) and Mongolia Gobi (Xu 2004; Zhang *et al.*, 2013). Here, we also previously indicated that local blowing dust could contribute to very high PM_{10} concentration. Additionally, the variations in B_{ap} and B_{sp} were generally consistent with the changes in PM_{10}. As an example, the values of B_{ap} and B_{sp} decreased from maximum values of 23.3 and 143 Mm^{-1} to minimum values of 11.3 and 50 Mm^{-1} with maximum/minimum ratios of around 2 and 3, respectively, during the morning of 10 April 2008, but the decreasing trends were smaller than that of the PM_{10} variation. While the dust event occurred, the increased SSA was consistent with the similar changes in PM_{10}. Similar results were obtained previously by Wang *et al.* (2015). Similar to Fig. 6, diurnal cycles of PM_{10}, B_{ap}, B_{sp}, and SSA are shown during local pollution episodes in Fig. 7. Comparing their optical properties, the pollution episodes could exist for a long period of time according to the local weather conditions. For instance, on 9 January 2008, the averaged PM_{10} concentration was 228 ± 50 μg m^{-3}, with a range of 108 to 301 μg m^{-3} and a valley that appeared at about 16:00. In contrast to the dust events, the value of B_{ap} was very sensitive to the variation in PM_{10} because of the large amount of light-absorbing impurities in the cold season, as we discussed in the previous section. On 6 January 2008, the PM_{10} concentration and B_{ap} decreased from 407 to 44 μg m^{-3} and from 90.9 to 9.4 Mm^{-1}, respectively. Additionally, the variation in B_{sp} showed the same trend as those in PM_{10} and B_{ap}. The variation in SSA had no significant trend corresponding to those of PM_{10}, B_{ap}, or B_{sp}. For instance, the variation trend of SSA was opposite that of PM_{10} on 6 January 2008, but it had a similar trend on 3 February 2008. The lowest value of SSA was 0.71 ± 0.03 on 9 January 2008, but SSA was almost always above 0.8 in the other cases.

Dust events and anthropogenic air pollution were two important weather conditions affecting local air quality at SACOL. To acquire deeper knowledge of the differences of aerosol size distribution and optical properties between dust events and anthropogenic pollution, a comparison was conducted (Fig. 8). The comparison of B_{ap} and PM_{10} is presented as six cases of pollution episodes (red dots) and dust events (black dots). The comparison shows a clear distinction of lower PM_{10} with higher B_{ap} for pollution episodes and higher PM_{10} with lower B_{ap} for dust events. The best fit of the slope could reflect the PM_{10} mass absorption efficiency and mass scattering efficiency (Ayers, 2001; Hammer *et al.*, 2001; Garland *et al.*, 2008). The slope of B_{ap}/PM_{10} was 0.132 for pollution episodes, much higher than the 0.008 for dust events, showing the markedly higher mass absorption efficiency of aerosols such as BC and OC in anthropogenic pollution. The correlation coefficient between B_{ap} and PM_{10} was $R^2 = 0.53$, suggesting more similar sources. As Fig. 6 shows, a dust event passed through SACOL from 16:00 to 23:00 on 29 February 2008. In the morning, the B_{ap} was around 15 Mm^{-1}, with a maximum of 20.7 Mm^{-1} before the dust storm occurred, but B_{ap} then decreased to a minimum of 3.5 Mm^{-1} followed by an increase of PM_{10} during the dust event. The B_{ap} then slowly increased to its peak (16.7 Mm^{-1}), which was close to its values in the morning. We note that the B_{ap} was dominated by mineral dust during the dust event of 29 February 2008 but that it was affected by the combined effects of dust storms and local pollution in other cases. The results indicate that mineral dust was dominant during a heavy dust event. Additionally, the mass absorption efficiency of dust and BC (mainly from local pollutants) is highly different (Zhang *et al.*, 2007; Yang *et al.*, 2009). As a result, mineral dust mixing with local pollutants led to a lower correlation coefficient between B_{ap} and PM_{10}. Similar to the case for B_{ap}, the slope of B_{sp}/PM_{10} was 0.61 during pollution episodes and 0.12 during dust events, reflecting the higher mass scattering efficiency of pollution events. The correlation coefficient between B_{sp} and PM_{10} of $R^2 = 0.21$ was lower than that for dust events (0,64), reflecting more complicated compositions of aerosols during the pollution episodes. A scatter plot of scattering aerosol efficiency (SAE) and absorption aerosol efficiency (AAE) is shown in Fig. 8(c). For dust events, the ranges of AAE and SAE were 1.25 to 1.75 and 1.0 to 2.5, respectively. Comparably, the ranges of AAE and SAE were mainly from 1.0 to 1.5 and 1.0 to 4.0, respectively, during pollution episodes. On 29 February 2008 and 8 May 2008, the PM_{10} was around 64 μg m^{-3} at13:00 and 119 μg m^{-3}, respectively, at

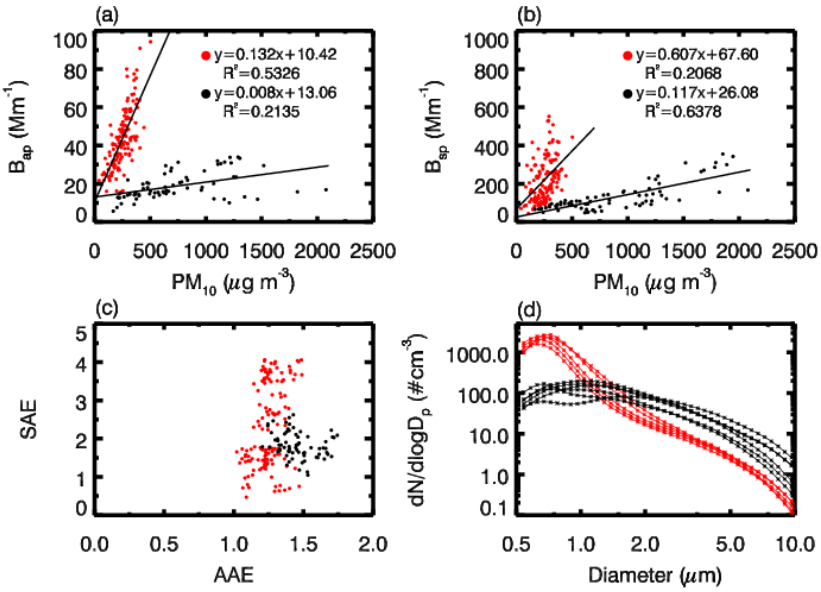

Fig. 8. Comparison of hourly aerosol optical properties and daily number concentration between dust events (black dots) and local air pollution events (red dots) at SACOL from March 2007 to December 2010.

14:00, before the dust event occurred. The PM_{10} concentration and AAE were in the ranges 1070–2080 μg m^{-3} and 1.55–1.74 (17:00–23:00) and 240–830 μg m^{-3} and 1.24–1.28 (15:00–19:00), respectively, during the dust events. The mixing ratios of local aerosols (including mainly local air pollutants) to aerosols during the dust events were 0.03–0.06 and 0.14–0.5. The results indicated that the AAE of mineral dust was beyond 1.5, which was similar to the results of Dubovik *et al.* (2002) and Russel *et al.* (2010). The values of AAE were much lower during air pollution than during dust events. However, there were slight changes in SAE due to the amount of mineral dust. As shown in Fig. 8(d), the peak value of $dN/dlogD_p$ for pollution events was up to 1500 # cm^{-3} at 0.7 μm. During dust events, the peak value was below 200 # cm^{-3} at around 1.0 μm (Sow *et al.*, 2009). The variation in $dN/dlogD_p$ was very small at diameters of 0.5–2.0 μm, as indicated by Sow *et al.* (2009). Large differences in $dN/dlogD_p$ between dust and air pollution events occurred at around 1.0–2.0 μm, and $dN/dlogD_p$ was ~10 times higher for fine-mode particles during air pollution events than during dust events.

CONCLUSIONS

In the field experiment, the average values of B_{sp}, B_{ap}, and PM_{10} concentration from March 2007 to December 2010 were 155 ± 102 Mm^{-1}, 16 ± 10 Mm^{-1}, and 120 ± 122 μg m^{-3}, respectively. The seasonal changes in PM_{10} were higher, with values of 121 ± 68 μg m^{-3} and 163 ± 199 μg m^{-3} in the cold season and spring season, respectively. The variations in B_{sp} and B_{ap} were much smaller compared with the changes in PM_{10}. The high values of B_{sp} and B_{ap} appeared in the cold season, with average values of 240 ± 145 Mm^{-1} and 26 ± 13 Mm^{-1}, respectively. The particle number concentration showed that both fine-mode and coarse-mode particles increased significantly in the cold season; however, the number concentration of fine-mode particles increased much more than that of coarse-mode particles.

The dust events occurred at various times of the day and lasted from several to dozens of hours. In contrast, the pollution episodes could exist for a long period of time, depending on the local weather conditions, and the B_{ap} was very sensitive to changes in PM_{10} during the air pollution events. The slopes of B_{ap}/PM_{10} and B_{sp}/PM_{10} could reflect the absorption and scattering properties of the aerosols. Generally, the slope of B_{ap}/PM_{10} was 0.132 for pollution episodes, which was much higher than the 0.008 value for dust events, showing markedly higher mass absorption efficiency for light-absorbing aerosols such as BC and OC originating from anthropogenic pollution. The correlation coefficient between B_{sp} and PM_{10} was higher during the dust (R^2 = 0.64) than during the air pollution events (R^2 = 0.21), reflecting the more complex compositions of the aerosols during the air pollution events during the cold season. In general, the dominant sources of PM_{10}, BC, and the other aerosol types in this region were obviously complex. We note that further field experiments for measuring dust events interacting with local pollutants near the dust sources are needed.

ACKNOWLEDGEMENTS

This research was supported by National Science Foundation of China under Grants 41175134 and 41105110, the Fundamental Research Funds for the Central Universities (lzujbky-2014-110 and lzujbky-2015-ct03), and the China 111 project (Grant No. B13045). Insightful comments offered by the two anonymous referees are highly appreciated. The English in this document has been checked by at least two professional editors, both native speakers of English. For a certificate, please see: http://www.textcheck.com/certificate/juRWua

REFERENCES

Allen, D., Pickering, K. and Fox-Rabinovitz, M. (2004). Evaluation of Pollutant Outflow and CO Sources during TRACE-P Using Model-calculated, Aircraft-based, and Measurements of Pollution in the Troposphere (MOPITT)-derived CO Concentrations. *J. Geophys. Res.* 109, doi: 10.1029/2003jd004250.

An, X.Q., Zuo, H.C. and Chen, L.J. (2007). Atmospheric Environmental Capacity of SO_2 in Winter over Lanzhou in China: A Case Study. *Adv. Atmos. Sci*. 24: 688–699.

Anderson, T.L., Masonis, S.J., Covert, D.S., Ahlquist, N.C., Howell, S.G., Clarke, A.D. and McNaughton, C.S. (2003). Variability of Aerosol Optical Properties Derived from in Situ Aircraft Measurements during ACE-Asia. *J. Geophys. Res.* 108: 8647, doi: 10.1029/2002JD003247.

Angstrom, A. (1929). On the Atmospheric Transmission of Sun Radiation and on Dust in the Air. *Geogr. Ann.* 11: 156–166.

Arimoto, R., Zhang, X.Y., Huebert, B.J., Kang, C.H., Savoie, D.L., Prospero, J.M., Sage, S.K., Schloesslin, C.A., Khaing, H.M. and Oh, S.N. (2004). Chemical Composition of Atmospheric Aerosols from Zhenbeitai, China, and Gosan, South Korea, during ACE-Asia. *J. Geophys. Res.* 109: D19S04, doi: 10.1029/2003JD004323.

Arimoto, R., Kim, Y.J., Kim, Y.P., Quinn, P.K., Bates, T.S., Anderson, T.L., Gong, S., Uno, I., Chin, M., Huebert, B.J., Clarke, A.D., Shinozuka, Y., Weber, R.J., Anderson, J.R., Guazzotti, S.A., Sullivan, R.C., Sodeman, D.A., Prather, K.A. and Sokolik, I.N. (2006). Characterization of Asian Dust during ACE-Asia. *Global Planet. Change* 52: 23–56.

Arnott, W.P., Hamasha, K., Moosmuller, H., Sheridan, P.J. and Ogren, J.A. (2005). Towards Aerosol Light-absorption Measurements with a 7-wavelength Aethalometer: Evaluation with a Photoacoustic Instrument and 3-wavelength Nephelometer. *Aerosol Sci. Technol.* 39: 17–29, doi: 10.1080/027868290901972.

Ayers, G.P. (2001). Comment on Regression Analysis of Air Quality Data. *Atmos. Environ.* 35: 2423–2425.

Bergin, M.H., Cass, G.R., Xu, J., Fang, C., Zeng, L.M., Yu, T., Salmon, L.G., Kiang, C.S., Tang, X.Y., Zhang, Y.H. and Chameides, W.L. (2001). (2001). Aerosol Radiative, Physical, and Chemical Properties in Beijing during June 1999. *J. Geophys. Res.* 106: 17969–17980.

Bi, J., Huang, J., Fu, Q., Ge, J., Shi, J., Zhou, T. and Zhang, W. (2013). Field Measurement of Clear-sky Solar Irradiance in BadainJaran Desert of Northwestern China. *J. Quant. Spectrosc. Radiat. Transfer* 122: 194–207.

Bi, J., Huang, J., Qiang, F., Wang, X., Shi, J., Zhang, W., Huang, Z. and Zhang, B. (2010). Toward Characterization of the Aerosol Optical Properties over Loess Plateau of Northwestern China. *J. Quant. Spectrosc. Radiat. Transfer* 112: D00K17, doi: 10.1029/2009JD013372.

Bi, J., Huang, J., Hu, Z., Holben, B. and Guo, Z. (2014). Investigating the Aerosol Optical and Radiative Characteristics of Heavy Haze Episodes in Beijing during January of 2013. *J. Geophys. Res.* 119: 9884–9900, doi: 10.1002/2014JD021757.

Cao, C.X., Zheng, S. and Singh, R.P. (2014). Characteristics of Aerosol Optical Properties and Meteorological Parameters during Three Major Dust Events (2005-2010) over Beijing, China. *Atmos. Res*. 150: 129–142.

Che, H., Wang, Y., Sun, J., Zhang, X., Zhang, X. and Guo, J. (2013). Variation of Aerosol Optical Properties over the Taklimakan Desert of China. *Aerosol Air Qual. Res.* 13: 777–785, doi: 10.4209/aaqr.2012.07.0200.

Che, H., Xia, X., Zhu, J., Li, Z., Dubovik, O., Holben, B., Goloub, P., Chen, H., Estelles, V., Cuevas-Agulló, E., Blarel, L., Wang, H., Zhao, H., Zhang, X., Wang, Y., Sun, J., Tao, R., Zhang, X. and Shi, G. (2014). Column Aerosol Optical Properties and Aerosol Radiative Forcing during a Serious Haze-fog Month over North China Plain in 2013 Based on Ground-based Sunphotometer Measurements. *Atmos. Chem. Phys*. 14: 2125–2138.

Chen, S., Huang, J., Zhao, C., Qian, Y., Leung, R. and Yang, B. (2013). Modeling the Transport and Radiative Forcing of Taklimakan Dust over the Tibetan Plateau: A Case Study in the Summer of 2006. *J. Geophys. Res.* 118, doi: 10.1002/jgrd.50122.

Chen, S., Zhao, C., Qian, Y., Leung, L., Huang, J., Huang, Z., Bi, J., Zhang, W., Shi, J., Yang, L., Li, D. and Li, J. (2014). Regional Modeling of Dust Mass Balance and Radiative Forcing over East Asia Using WRF-Chem. *Aeolian Res.* 15: 15–30, doi: 10.1016/j.aeolia.2014.02.001.

Conant, W.C., Seinfeld, J.H., Wang, J., Carmichael, G.R., Tang, Y.H., Uno, I., Flatau, P.J., Markowicz, K.M. and Quinn, P.K. (2003). A Model for the Radiative Forcing during ACE-Asia Derived from CIRPAS Twin Otter and R/V Ronald H. Brown Data and Comparison with Observations. *J. Geophys. Res.* 108: 8661, doi: 10.1029/2002JD003260.

Costabile, F., Bertoni, G., De Santis, F., Bellagotti, R., Ciuchini, C., Vichi, F. and Allegrini, I. (2010). Spatial Distribution of Urban Air Pollution in Lanzhou, China. *Open Environ. Pollut. Toxicol. J.* 2: 8–15.

Draxier, R.R. and Hess, G.D. (1998). An Overview of the HYSPLIT_4 Modelling System for Trajectories, Dispersion and Deposition. *Aust. Meteorol. Mag.* 47: 295–308.

Draxler, R.R. and Rolph, G.D. (2008). HYSPLIT (HYbrid Single-PartilceLagrangian Integrated Trajectory), http://www.arl.noaa.gov/ready/hysplit4.html.

Dubovik, O., Holben, B.N., Eck, T.F., Smirnov, A., Kaufman, Y.J., King, M.D., Tanré, D. and Slutsker, I. (2002). Variability of Absorption and Optical Properties of Key Aerosol Types Observed in Worldwide Locations. *J. Atmos. Sci.* 59: 590–608.

Fialho, P., Hansen, A.D.A. and Honrath, R.E. (2005). Absorption Coefficients by Aerosols in Remote Areas: A New Approach to Decouple Dust and Black Carbon Absorption Coefficients Using Seven-wavelength Aethalometer Data. *J. Aerosol Sci.* 36: 267–282.

Fu, Q., Thorsen, T.J., Su, J., Ge, J.M. and Huang, J.P. (2009). Test of Mie-based Single-scattering Properties of Non-spherical Dust Aerosols in Radiative Flux Calculations. *J. Quant. Spectrosc. Radiat. Transfer* 110: 1640–1653.

Garland, R.M., Yang, H., Schmid, O., Rose, D., Nowak,

A., Achtert, P., Wiedensohler, A., Takegawa, N., Kita, K., Miyazaki, Y., Kondo, Y., Hu, M., Shao, M., Zeng, L. M., Zhang, Y.H., Andreae, M.O. and Pöschl, U. (2008). Aerosol Optical Properties in a Rural Environment near the Mega-city Guangzhou, China: Implications for Regional Air Pollution, Radiative Forcing and Remote Sensing. *Atmos. Chem. Phys.* 8: 5161–5186.

Gong, S.L., Zhang, X.Y., Zhao, T.L., McKendry, I.G., Jaffe, D.A. and Lu, N.M. (2003). Characterization of Soil Dust Aerosol in China and Its Transport and Distribution during 2001 ACE-Asia: 2. Model Simulation and Validation. *J. Geophys. Res.* 108: 1984–2012.

Hammer, Ø., Harper, D.A.T. and Ryan, P.D. (2001). PAST: PaleontologicalStatistics Software Package for Education and Data Analysis. *Palaeontol. Electronica* 4: 1–9.

Hegg, D.A., Warren, S.G., Grenfell, T.C., Doherty, S.J., Larson, T.V. and Clarke, A.D. (2009). Source Attribution of Black Carbon in Arctic Snow. *Environ. Sci. Technol.* 43: 4016–4021.

Hegg, D.A., Warren, S.G., Grenfell, T.C., Doherty, S.J. and Clarke, A.D. (2010). Sources of Light-absorbing Aerosol in Arctic Snow and Their Seasonal Variation. *Atmos. Chem. Phys.* 10: 10923–10938.

Hitzenberger, R. and Tohno, S. (2001). Comparison of Black Carbon (BC) Aerosols in Two Urban Areas–concentrations and Size Distributions. *Atmos. Environ.* 35: 2153–2167.

Huang, J., Lin, B., Minnis, P., Wang, T., Wang, X., Hu, Y., Yi, Y. and Ayers, J.R. (2006a). Satellite-based Assessment of Possible Dust Aerosols Semi-direct Effect on Cloud Water Path over East Asia. *Geophys. Res. Lett.* 33, doi: 10.1029/2006GL026561.

Huang, J., Minnis, P., Lin, B., Wang, T., Yi, Y., Hu, Y., Sun-Mack, S. and Ayers, K. (2006b). Possible Influences of Asian Dust Aerosols on Cloud Properties and Radiative Forcing Observed from MODIS and CERES. *Geophys. Res. Lett.* 33: L06824, doi: 10.1029/2005GL024724.

Huang, J., Minnis, P., Chen, B., Huang, Z., Liu, Z., Zhao, Q., Yi, Y. and Ayers, J.K. (2008a). Long-range Transport and Vertical Structure of Asian Dust from CALIPSO and Surface Measurements during PACDEX. *J. Geophys. Res.* 113: D23212, doi: 10.1029/2008JD010620.

Huang, J., Zhang, W., Zuo, J., Bi, J., Shi, J., Wang, X., Chang, Z., Huang, Z., Yang, S., Zhang B., Wang, G., Feng, G., Yuan, J., Zhang, L., Zuo, H., Wang, S., Fu, C. and Chou, J. (2008b). An Overview of the Semi-Arid Climate and Environment Research Observatory over the Loess Plateau. *Adv. Atmos. Sci.* 25: 1–16.

Huang, J., Fu, Q., Zhang, W., Wang, X., Zhang, R., Ye, H. and Warren, S.G. (2011). Dust and Black Carbon in Seasonal Snow across Northern China. *Bull. Am. Meteorol. Soc.* 92: 175–181.

Huang, J., Wang, T., Wang, W., Li, Z. and Yan, H. (2014). Climate Effects of Dust Aerosols over East Asian Arid and Semiarid Regions. *J. Geophys. Res.* 119: 11398–11416, doi: 10.1002/2014JD021796.

Huang, Z., Huang, J., Bi, J., Wang, G., Wang, W., Fu, Q., Li, Z., Tsay, S.C. and Shi, J. (2010). Dust Aerosol Vertical Structure Measurements Using Three MPL Lidars during 2008 China-U.S. Joint Dust Field Experiment. *J. Geophys. Res.* 115: D00K15, doi: 10.1029/2009JD013273.

Huebert, B.J., Bates, T., Russell, P.B., Shi, G.Y., Kim, Y.J., Kawamura, K., Carmichael, G. and Nakajima, T. (2003). An Overview of ACE-Asia: Strategies for Quantifying the Relationships between Asian Aerosols and Their Climatic Impacts. *J. Geophys. Res.* 108: 8633, doi: 10.1029/2003JD003550.

Hyvärinen, A.P., Kolmonen, P., Kerminen, V.M., Virkkula, A., Leskinen, A., Komppula, M., Hatakka, J., Burkhart, J., Stohl, A., Aalto, P., Kulmala, M., Lehtinen, K.E.J., Viisanen, Y. and Lihavainen, H. (2011). Aerosol Black Carbon at Five Background Measurement Sites over Finland, a Gateway to the Arctic. *Atmos. Environ.* 45: 4042–4050.

Igarashi, Y., Fujiwara, H. and Jugder, D. (2011). Change of the Asian Dust Source Region Deduced from the Composition of Anthropogenic Radionuclides in Surface Soil in Mongolia. *Atmos. Chem. Phys*. 11: 7069–7080.

IPCC (2013). Climate Change, 2013: The Physical Science Basis. Contribution of Working Group I to the Fifth Assessment Report of the Intergovernmental Panel on Climate Change. Cambridge University Press, Cambridge, United Kingdom and New York, NY, USA.

Jacob, D.J., Crawford, J.H., Kleb, M.M., Connors, V.S., Bendura, R.J., Raper, J.L., Sachse, G.W., Gille, J.C., Emmons, L. and Heald, C.L. (2003). Transport and Chemical Evolution over the Pacific (TRACE-P) Aircraft Mission: Design, Execution, and First Results. *J. Geophys. Res.* 108, doi: 10.1029/2002JD003276.

Jaffe, D., Anderson, T., Covert, D., Kotchenruther, R., Trost, B., Danielson, J., Simpson, W., Berntsen, T., Karlsdottir, S., Blake, D., Harris, J., Carmichael, G. and Uno, I. (1999). Transport of Asian Air Pollution to North America. *Geophys. Res. Lett.* 26: 711–714.

Jing, J.S., Wu, Y.F., Tao, J., Che, H.Z., Xia, X.G., Zhang, X.C., Yan, P., Zhao, D.M. and Zhang, L.M. (2015). Observation and Analysis of Near-surface Atmospheric Aerosol Optical Properties in Urban Beijing. *Particuology* 18: 144–154.

Kalkstein, L.S., Tan, G. and Skindlov, J.A. (1987). An Evaluation of Three Clustering Procedures for Use in Synoptic Climatological Classification. *J. Climate Appl. Meteorol.* 26: 717–730.

Kim, S.W., Jefferson, A., Yoon, S C., Dutton, E.G., Ogren, J.A., Valero, F.P.J., Kim, J. and Holben, B.N. (2005). Comparisons of Aerosol Optical Depth and Surface Shortwave Irradiance and Their Effect on the Aerosol Surface Radiative Forcing Estimation. *J. Geophys. Res.* 110: D07204, doi: 10.1029/2004JD004989.

Li, Z., Li, C., Chen, H., Tsay, S.C., Holben, B., Huang, J., Li, B., Maring, H., Qian, Y., Shi, G., Xia, X., Yin, Y., Zheng, Y. and Zhuang, G. (2011). East Asian Studies of Tropospheric Aerosols and Their Impact on Regional Climate (EAST-AIRC): An overview. *J. Geophys. Res.* 116: D00K34, doi: 10.1029/2010JD015257.

Li, C., Marufu, L.T., Dickerson, R.R., Li, Z., Wen, T., Wang, Y., Wang, P., Chen, H. and Stehr, J.W. (2007). In Situ Measurements of Trace Gases and Aerosol Optical

Properties at a Rural Site in northern China during East Asian Study of Tropospheric Aerosols: An International Regional Experiment 2005. *J. Geophys. Res.* 112: D22S04, doi: 10.1029/2006JD007592.

Li, C., Tsay, S.-C., Fu, J.S., Dickerson, R.R., Ji, Q., Bell, S.W., Gao, Y., Zhang, W., Huang, J., Li, Z. and Chen, H. (2010). Anthropogenic Air Pollution Observed near Dust Source Regions 785 in Northwestern China during Springtime 2008. *J. Geophys. Res.* 115: D00K22, doi: 10.1029/2009JD013659.

Littmann, T. (1991). Dust Storm Frequency in Asia-climatic Control and Variability. *Int. J. Climatol.* 11: 393–412.

Liu, Y., Huang, J., Shi, G., Takamura, T., Khatri, P., Bi, J., Shi, J., Wang, T., Wang, X. and Zhang, B. (2011). Aerosol Optical Properties and Radiative Effect Determined from Sky-radiometer over Loess Plateau of Northwest China. *Atmos. Chem. Phys.* 11: 11455–11463.

Mari, C., Evans, M.J., Palmer, P.I., Jacob, D.J. and Sachse, G.W. (2004). Export of Asian Pollution during Two Cold Front Episodes of the TRACE-P Experiment. *J. Geophys. Res.* 109, doi: 10.1029/2003jd004307.

Marinoni, A., Cristofanelli, P., Calzolari, F., Roccato, F., Bonafè, U. and Bonasoni, P. (2008). Continuous Measurements of Aerosol Physical Parameters at the Mt. Cimone GAW Station (2165 m asl, Italy). *Sci. Total Environ.* 391: 241–251.

McKendry, I.G., Macdonald, A.M., Leaitch, W.R., Donkelaar, A., Zhang, Q., Duck, T. and Martin, R.V. (2008). Trans-Pacific Dust Events Observed at Whistler, British Columbia during INTEX-B. *Atmos. Chem. Phys.* 8: 6297–6307, doi: 10.5194/acp-8-6297-2008.

Mori, I., Nishikawa, M., Tanimura, T. and Quan, H. (2003). Change in Size Distribution and Chemical Composition of Kosa (Asian dust) Aerosol during Long-range Transport. *Atmos. Environ.* 37: 4253–4263.

Petzold, A., Kopp, C. and Niessner, R. (1997). The Dependence of the Specific Attenuation Cross-section on Black Carbon Mass Fraction and Particle size. *Atmos. Environ.* 31: 661–672.

Prospero, J.M. (1999). Long-term Measurements of the Transport of African Mineral Dust to the Southeastern United States: Implications for Regional Air Quality. *J. Geophys. Res.* 104: 15917–15927.

Prospero, J.M. and Mayol-Bracero, O.L. (2013). Understanding the Transport and Impact of African Dust on the Caribbean Basin. *Bull. Am. Meteorol. Soc.* 94: 1329–1337.

Ramanathan, V., Crutzen, P.J., Kiehl, J.T. and Rosenfeld, D. (2001a). Atmosphere - Aerosols, Climate, and the Hydrological Cycle. *Science* 294: 2119–2124.

Ramanathan, V., Crutzen, P.J., Lelieveld, J., Mitra, A.P., Althausen, D., Anderson, J., Andreae, M.O., Cantrell, W., Cass, G.R., Chung, C.E., Clarke, A.D., Coakley, J.A., Collins, W.D., Conant, W.C., Dulac, F., Heintzenberg, J., Heymsfield, A.J., Holben, B., Howell, S., Hudson, J., Jayaraman, A., Kiehl, J.T., Krishnamurti, T.N., Lubin, D., McFarquhar, G., Novakov, T., Ogren, J.A., Podgorny, I.A., Prather, K., Priestley, K., Prospero, J.M., Quinn, P.K., Rajeev, K., Rasch, P., Rupert, S., Sadourny, R., Satheesh, S.K., Shaw, G.E., Sheridan, P. and Valero, F.P.J. (2001b). Indian Ocean Experiment: An Integrated Analysis of the Climate Forcing and Effects of the Great Indo-Asian Haze. *J. Geophys. Res.* 106: 28371–28398.

Ramanathan, V., Chung, C., Kim, D., Bettge, T., Buja, L., Kiehl, J.T., Washington, W.M., Fu, Q., Sikka, D.R. and Wild, M. (2005). Atmospheric Brown Clouds: Impacts on South Asian Climate and Hydrological Cycle. *Proc. Nat. Acad. Sci. U.S.A.* 102: 5326–5333.

Ramanathan, V. and Carmichael, G. (2008). Global and Regional Climate Changes Due to Black Carbon. *Nat. Geosci.* 1: 221–227.

Rosenfeld, D., Rudich, Y. and Lahav, R. (2001). Desert Dust Suppressing Precipitation: A Possible Desertification Feedback Loop. *Proc. Nat. Acad. Sci. U.S.A.* 98: 5975–5980.

Russell, P.B., Bergstrom, R.W., Shinozuka, Y., Clarke, A.D., DeCarlo, P.F., Jimenez, J.L., Livingston, J.M., Redemann, J., Dubovik, O. and Strawa, A. (2010). Absorption Angstrom Exponent in AERONET and Related Data as an Indicator of Aerosol Composition. *Atmos. Chem. Phys.* 10: 1155–1169.

Sow, M., Alfaro, S.C., Rajot, J.L. and Marticorena, B. (2009). Size Resolved Dust Emission Fluxes Measured in Niger during 3 Dust Storms of the AMMA Experiment. *Atmos. Chem. Phys.* 9: 3881–2009.

Stunder, B. (1997). FNL Readme File, http://www.arl.noaa.gov/ready-bin/fnl.pl.

Su, J., Huang, J.P., Fu, Q., Minnis, P., Ge, J.M. and Bi, J.R. (2008). Estimation of Asian Dust Aerosol Effect on Cloud Radiation Forcing Using Fu-Liou Radiative Model and CERES Measurements. *Atmos. Chem. Phys.* 8: 2763–2771.

Sullivan, R.C., Guazzotti, S.A., Sodeman, D.A. and Prather, K.A. (2007). Direct Observations of the Atmospheric Processing of Asian Mineral Dust. *Atmos. Chem. Phys.* 7: 1213–1236.

Sun, Y., Zhuang, G., Wang, Y., Zhao, X., Li, J., Wang, Z. and An, Z. (2005). Chemical Composition of Dust Storms in Beijing and Implications for the Mixing of Mineral Aersol with Pollution Aerosol on the Pathway. *J. Geophys. Res.* 110: D24209, doi: 10.1029/2005JD006054.

Tegen, I., Lacis, A.A. and Fung, I. (1996). The Influence on Climate Forcing of Mineral Aerosols from Disturbed Soils. *Nature* 380: 419–422.

Tu, F.H., Thornton, D.C., Bandy, A.R., Kim, M., Carmichael, G., Tang, Y., Thornhill, L. and Sachse, G. (2003). Dynamics and Transport of Sulfur Dioxide over the Yellow Sea during TRACE-P. *J. Geophys. Res.* 108: 8790, doi: 10.1029/2002JD003227.

VanCuren, R.A. and Cahill, T.A. (2002). Asian Aerosols in North America: Frequency and Concentration of fine Dust. *J. Geophys. Res.* 107: 1984–2012.

Wang, T., Wong, C.H., Cheung, T.F., Blake, D.R., Baumann, K., Arimoto, R., Baumann, K., Tang, J., Ding, G.A., Yu, X.M., Li, Y.S., Streets, D.G. and Simpson, I.J. (2004). Relationships of Trace Gases and Aerosols and the Emission Characteristics at Lin'an, a Rural site in Eastern China, during Spring 2001. *J. Geophys. Res.* 109: D19S05,

doi: 10.1029/2003JD004119.

Wang, X., Huang, J.P., Ji, M.X. and Higuchi, K. (2008). Variability of East Asia Dust Events and Their Long-term Trend. *Atmos. Environ.* 42: 3156–3165.

Wang, X., Huang, J.P., Zhang, R.D., Chen, B. and Bi, J (2010). Surface Measurements of Aerosol Properties over Northwest China during ARM China 2008 Deployment. *J. Geophys. Res.* 115: D00K27, doi: 10.1029/2009JD013467.

Wang, X., Doherty, S.J. and Huang, J.P. (2013). Black Carbon and Other Light-absorbing Impurities in Snow across Northern China. *J. Geophys. Res.* 118: 1471–1492.

Wang, X., Pu, W., Shi, J., Bi, J., Zhou, T., Zhang, X. and Ren, Y. (2015). A Comparison of the Physical and Optical Properties of Anthropogenic air Pollutants and Mineral Dust over Northwest China. *J. Meteorol. Res.* 29: 180–200, doi: 10.1007/s13351-015-4092-0.

Woo, J.H., Streets, D.G., Carmichael, G.R., Tang, Y.H., Yoo, B., Lee, W.C., Thongboonchoo, N., Pinnock, S., Kurata, G., Uno, I., Fu, Q., Vay, S., Sachse, G.W., Blake, D.R., Fried, A. and Thorton, D.C. (2003). Contribution of Biomass and Biofuel Emissions to Trace Gas Distributions in Asia during the TRACE-P Experiment. *J. Geophys. Res.* 108: 8812, doi: 10.1029/2002JD003200.

Xu, J., Bergin, M.H., Greenwald, R., Schauer, J.J., Shafer, M.M., Jaffrezo, J.L. and Aymoz, G. (2004). Aerosol Chemical, Physical, and Radiative Characteristics near a Desert Source Region of Northwest China during ACE-Asia. *J. Geophys. Res.* 109: D19S03, doi: 10.1029/2003JD004239.

Yang, M., Howell, S.G., Zhuang, J. and Huebert, B.J. (2009). Attribution of Aerosol Light Absorption to Black Carbon, Brown Carbon, and Dust in China - Interpretations of Atmospheric Measurements during EAST-AIRE. *Atmos. Chem. Phys.* 9: 2035–2050.

Yuan, H., Zhuang, G., Li, J., Wang, Z. and Li, J. (2008). Mixing of Mineral with Pollution Aerosols in Dust Season in Beijing: Revealed by Source Apportionment Study. *Atmos. Environ.* 42: 2141–2157.

Zhang, Q., Streets, D.G., Carmichael, G.R., He, K.B., Huo, H., Kannari, A., Klimont, Z., Park, I.S., Reddy, S., Fu, J.S., Chen, D., Duan, L., Lei, Y., Wang, L.T. and Yao, Z.L. (2009). Asian Emissions in 2006 for the NASA INTEX-B Mission. *Atmos. Chem. Phys.* 9: 5131–5153, doi: 10.5194/acp-9-5131-2009.

Zhang, Q. and Li, H.Y. (2011). A Study of the Relationship between Air Pollutants and Inversion in the ABL over the City of Lanzhou. *Adv. Atmos. Sci*. 28: 879–886.

Zhang, R.J., Cao, J.J., Lee, S.C., Shen, Z.X. and Ho, K.F. (2007). Carbonaceous Aerosols in PM_{10} and Pollution Gases in Winter in Beijing. *J. Environ. Sci.* 19: 564–571.

Zhang, R., Hegg, D.A., Huang, J. and Fu, Q. (2013). Source Attribution of Insoluble Light-absorbing Particles in Seasonal Snow across Northern China. *Atmos. Chem. Phys.* 13: 6091–6099.

Zhang, X.Y., Gong, S.L., Arimoto, R., Shen, Z.X., Mei, F.M., Wang, D. and Cheng, Y. (2003a). Characterization and Temporal Variation of Asian Dust Aerosol from a Site in the northern Chinese Deserts. *J. Atmos. Chem.* 44: 241–257.

Zhang, X.Y., Gong, S.L., Shen, Z.X., Mei, F.M., Xi, X.X., Liu, L.C., Zhou, Z.J., Wang, D., Wang, Y.Q. and Cheng, Y. (2003b). Characterization of Soil Dust Aerosol in China and Its Transport and Distribution during 2001 ACE-Asia: 1. Network Observations. *J. Geophys. Res.* 108.

Zhao, T.L., Gong, S.L., Zhang, X.Y. and Jaffe, D.A. (2008). Asian Dust Storm Influence on North American Ambient PM Levels: Observational Evidence and Controlling Factors. *Atmos. Chem. Phys.* 8: 2717–2728.

Zheng, S., Wang, M.Z., Wang, S.G., Tao, Y. and Shang, K.Z. (2013). Short-Term Effects of Gaseous Pollutants and Particulate Matter on Daily Hospital Admissions for Cardio-Cerebrovascular Disease in Lanzhou: Evidence from a Heavily Polluted City in China. *Int. J. Environ. Res. Public Health* 10: 462–477.

Zhou, T., Huang, J.P., Huang, Z.W., Liu, J.J., Wang, W.C. and Lin, L. (2013). The Depolarization-attenuated Backscatter Relationship for Dust Plumes. *Opt. Express* 13: 15195–15204, doi: 10.1364/OE.21.015195.

Received for review, February 23, 2015
Revised, May 7, 2015
Accepted, May 7, 2015